XCP1 is a caspase that proteolyzes Pathogenesis-related protein 1 to produce the cytokine CAPE9 for systemic immunity in *Arabidopsis*

Ying-Lan Chen
Academia Sinica
Fan-Wei Lin
Academia Sinica
Kai-Tan Cheng
Academia Sinica
Hung-Yu Wang
Academia Sinica
Thomas Efferth
Johannes Gutenberg University
Yet-Ran Chen (yetran@gate.sinica.edu.tw)
Academia Sinica https://orcid.org/0000-0002-2409-6655

Article

Keywords: Plant Immunity, Systemic Acquired Resistance, Caspase, Peptide Cytokine, Protease, Salicylic Acid

Posted Date: February 15th, 2021

DOI: https://doi.org/10.21203/rs.3.rs-155784/v1

Abstract

Proteolytic activation of cytokines regulates immunity in diverse organisms. In animals, cysteine-dependent aspartate-specific proteases (caspases) play central roles in cytokine maturation. Although the proteolytic production of peptide cytokines is also essential for plant immunity, evidence for a plant caspase is still lacking. In this study, we discovered that proteolysis of a caspase-like substrate motif “CNYD” within Pathogenesis-related protein 1 (AtPR1) in Arabidopsis generates an immunomodulatory cytokine (AtCAPE9). Salicylic acid enhances CNYD-targeted protease activity and the proteolytic release of AtCAPE9 from AtPR1 in Arabidopsis. We show that this process involves a caspase, identified as Xylem cysteine peptidase 1 (XCP1). XCP1 exhibits a calcium-modulated pH-activity profile and a comparable activity to human caspases. XCP1 is required to induce systemic immunity triggered by pathogen-associated molecular patterns. This work reveals XCP1 as the first known plant caspase, which produces the cytokine AtCAPE9 from the canonical salicylic acid signaling marker PR1 to activate systemic immunity.

Introduction

Proteases, which hydrolyze proteins into shorter proteins, peptides or amino acids, are involved not only in protein turnover but also in the regulation of diverse physiological events[1]. For instance, proteases regulate immunity by generating peptides from host or pathogen precursors; these peptides activate and orchestrate defense responses to defeat biological threats[2]. In the animal kingdom, members of the cysteine-dependent aspartate-specific protease (caspase) family serve as central mediators in the initiation and execution of apoptosis, as well as the activation of inflammation via proteolytic maturation of cytokines[3]. Caspases belong to a cysteine protease family with high specificity; they recognize a motif of at least four amino acids that ends in and cleaves immediately after aspartate (xxxD↓x)[4]. Although plants are expected to have caspases[5], no sequence homologue of caspases has been directly identified[6], and no plant protease has been found to cleave a precursor after aspartate to produce a mature cytokine directly. Currently, the only known functional analogs of animal caspases in plants are metacaspases (a type of cysteine protease that cleaves lysine/arginine) and phytaspases (a type of serine proteases that cleaves aspartate)[7, 8]. Although caspase-like activity has been reported in plants[9], and plant immune responses can be initiated by the maturation of plant immunomodulatory peptide cytokines[10], the underlying caspases are not clear.

Among the known immunomodulatory peptides in plants, a tomato wound-induced peptide is produced by cleavage event that is after a caspase-like substrate motif, “CNYD↓”, within the proprotein “Pathogenesis-related protein 1” (PR1)[11]. PR1 belongs to the cysteine-rich secretory protein, antigen 5, and pathogenesis-related 1 protein (CAP) superfamily[12], thus the first identified mature peptide was named CAP-derived peptide 1 (CAPE1)[13]. Tomato CAPE1 (SlCAPE1) induces antipathogen and minor antiherbivore responses, without significantly triggering programmed cell death. SlCAPE1, and the CNYD domain positioned N-terminal to SlCAPE1, are highly conserved within PR1 across diverse plant species.

PR1 is the most common marker for salicylic acid-regulated plant immunity and its secretion is critical for the activation of systemic acquired resistance (SAR) in *Arabidopsis*[14]. Nevertheless, how PR1 regulates SAR is poorly understood. In *Arabidopsis*, CAPE9 (AtCAPE9) is a putative CAPE that is also derived from PR1 (AtPR1), and treatment with synthetic AtCAPE9 induces antipathogen activity in *Arabidopsis*[13]. However, endogenous AtCAPE9 has not yet been detected, and whether AtPR1 is proteolytically processed to regulate plant systemic immunity is unknown. To uncover a potential role for AtPR1 proteolysis in the activation of SAR, we aimed to identify AtCAPE9 and its corresponding protease.

Results

AtCAPE9 is generated from aspartate-specific proteolysis of AtPR1 and enhances immunity in *Arabidopsis*

To decipher the function of AtCAPE9 in regulating *Arabidopsis* immunity, we treated two groups of *Arabidopsis* plants with water or an aqueous solution of synthetic AtCAPE9 (PRGNYVNEKPY). Compared to plants treated with water, those treated with AtCAPE9 displayed an increased level of salicylic acid (SA) (3.3-fold) and reduced infection upon inoculation with *Pseudomonas syringae pv.* tomato DC3000 (*Pst* DC3000)[11] (72.5-fold in this study) (Fig. 1a). We performed LC-MS/MS to identify AtCAPE9 in SA-treated leaves and detected endogenous AtCAPE9, whose MS/MS spectrum closely matched that of synthetic AtCAPE9 (Fig. 1b). Thus, AtCAPE9 is an endogenous peptide cytokine that can regulate SA levels and enhances pathogen resistance.

To investigate AtPR1 processing is depending on the aspartate of CNYD motif that is N-terminal to the AtCAPE9 sequence in AtPR1, we expressed a series of modified AtPR1 sequences fused to enhanced yellow fluorescent protein (eYFP) in *Arabidopsis.* Specifically, we examined native (N, CNYDP) or alanine-substituted versions (D150A: CNYAP or P151A: CNYDA) of AtPR1-eYFP (Fig. 1c). We detected a ~44.7 kDa protein with all three constructs, corresponding to intact (uncleaved) AtPR1-eYFP. In contrast, the putative AtCAPE9-eYFP cleavage product (~27.0 kDa) was produced from AtPR1-eYFP of the native and P151A mutant, but not from the D150A mutant. These data suggest that the aspartate in the potential caspase substrate domain CNYD is important for AtPR1 cleavage.

SA increases AtCAPE9 level, AtPR1-eYFP cleavage and CNYD-targeted protease (CNYDase) activity in *Arabidopsis*

We hypothesized that AtCAPE9, like AtPR1, is involved in SA-triggered immunity in *Arabidopsis*. To determine if SA treatment induces the production of AtCAPE9, we used LC-MS/MS to quantify the level of endogenous AtCAPE9 in plants with or without SA treatment. Briefly, LC-MS/MS was operated in selected reaction monitoring (SRM) mode targeting the fragmentation transitions of AtCAPE9. We found that the level of AtCAPE9 was ~6-fold higher in SA-treated plants compared to the untreated controls (Fig. 2a). Moreover, the levels of AtCAPE9-eYFP produced from AtPR1-eYFP were higher in transgenic plants

treated with SA or the SA functional analogue 2,6-dichloroisonicotinic acid (INA) compared to mock-treated controls (Fig. 2b).

To monitor CNYDase activity, we incubated a fluorogenic protease substrate Ac-CNYD-AMC (Fig. S1) with plant extract. Substrate cleavage was elevated in extracts from SA-treated and INA-treated plants, compared to extracts from mock-treated or wounded plants (Fig. 2c), suggesting that CNYDase activity increases upon SA and INA treatment. Together, these data suggest that SA treatment enhances CNYDase activity to generate increased level of AtCAPE9 from AtPR1 in *Arabidopsis*.

Identification of a putative caspase targeting the CNYD motif in *Arabidopsis*

Next, we used the CNYDase assay to further examine whether the conserved CNYD motif in AtPR1 is essential for proteolytic release of AtCAPE9. Indeed, we observed substantially reduced cleavage of fluorogenic substrates with a disrupted CNYD motif (Ac-CNAD-AMC, Ac-ANAD-AMC) compared to the canonical Ac-CNYD-AMC substrate (Fig. 3a). In addition, cleavage of the Ac-CNYD-AMC substrate was significantly enhanced by $CaCl_2$, but inhibited by $ZnCl_2$ and the metal chelator EDTA, as compared to the control (Fig. 3b; left panel). The Ca^{2+}-enhanced CNYDase activity was strongly suppressed by a general cysteine protease inhibitor (E-64) or a biotinylated aldehyde tetrapeptide CNYD (biotin-CNYD-CHO; Fig. S1, Fig. 3b; right panel). The suppression by E-64 suggested that the CNYDase is a cysteine protease that catalyzes a cysteine-dependent proteolytic reaction.

The biotin-CNYD-CHO inhibitor was designed to probe and covalently modify the cysteine in the active site of CNYDases, and displayed dose-dependent inhibition of CNYDase activity with the Ac-CNYD-AMC substrate (Fig. 3c; left panel). We incubated biotin-CNYD-CHO with wild-type (WT) *Arabidopsis* extract, and detected biotin-CNYD-CHO-labelled proteins with streptavidin-HRP by western blotting. Intriguingly, we observed prominent labeling of a potential 35 kDa CNYDase and two minor protein bands at 64 and 24 kDa (Fig. 3c; right panel). Together, our results so far point to a protease that is mainly 35 kDa, Ca^{2+}-activated cysteine-dependent aspartate-specific CNYDase (caspase) in *Arabidopsis*.

XCP1 is a CNYDase enzyme specific for CAPE production from AtPR1

To discover the enzyme specific for CAPE production (designated ESCAPE), we investigated two cysteine protease families in *Arabidopsis*, the papain-like cysteine proteases (PLCPs) and metacaspases (MCs), which have caspase-like functions in regulating plant immunity and programmed cell death[15, 16]. The MC family members are not aspartate-specific and therefore were excluded as candidates. Among the 31 *Arabidopsis* PLCPs, we identified ESCAPE candidates that had: (1) a molecular weight of 34.00-37.00 kDa (untruncated, pro-form) and 23.00-25.00 kDa (truncated, processed form) (Table S1), and (2) an expression pattern that correlates with *AtPR1* expression during leaf development[17] (Fig. S2). The only *PLCP* that fit both criteria was Xylem cysteine peptidase 1 (XCP1; At4g35350), which is a member of PLCP subfamily III (Fig. S3a). In addition, the ~35 kDa untruncated form of XCP1 is significantly more abundant than the ~23 kDa truncated form in 35S:XCP1 plants[18].

To examine the potential CNYDase activity of XCP1, we used the *xcp1* T-DNA insertion mutant (SALK_084789), which we confirmed by genotyping and gene expression (Fig. S3b-d). We observed significantly lower CNYDase activity in lysate from the *xcp1* mutant compared to from WT and other *PLCP* mutants (Fig. S4). Moreover, biotin-CNYD-CHO did not label any proteins in *xcp1* mutant extract, unlike WT (Fig. 4a). Together these data suggest that XCP1 directly recognizes the CNYD motif and catalyzes a proteolytic reaction on the aspartate.

To further investigate the activity of XCP1, we expressed and affinity purified an XCP1-His fusion protein from tobacco leaves. The expected molecular weights of the untruncated and truncated XCP1-His proteins are 37.6 kDa and 24.6 kDa, respectively (Figure S5a), and we detected purified His-tagged proteins of 45 kDa, 32-37 kDa and 25 kDa by immunoblotting (Figure S5b). The 45 kDa protein has been suggested to be a preprotein form of XCP1, which can be observed when the protein is overexpressed[18]. Among the different forms of the XCP1-His protein that were expressed and purified from tobacco, the 34-36 kDa and 25 kDa forms could be labeled by biotin-CNYD-CHO (Figure S5b), suggesting that these forms are active CNYDases. Purified XCP1-His displayed proteolytic activity with the Ac-CNYD-AMC substrate, but not with the Ac-CNAD-AMC nor Ac-ANAD-AMC substrates, and this activity was efficiently inhibited by co-incubation with biotin-CNYD-CHO (Fig. 4b). Moreover, the CNYDase activity of purified XCP1-His was enhanced by $CaCl_2$ and inhibited by $ZnCl_2$ and E-64, and slightly reduced by EDTA as compared to the control (Fig. 4c), similar to our observations with WT *Arabidopsis* lysate. We found that purified XCP1-His exhibited the highest CNYDase activity at pH 6.0 in the presence of excess $CaCl_2$, and at pH 5.0 in the absence of excess $CaCl_2$ (Fig. 4d). In addition, purified XCP1-His (1 µg) was substantially more active at 22 °C as compared to 32 °C and 37 °C (Fig. S6). At 22 °C, purified XCP1-His (0.2 µg) cleaved Ac-CNYD-AMC with a K_m of ~26.5 µM and V_{max} of ~251.2 RFU/min (Fig. 4e). To determine whether the cysteine (C161) in the putative active site of XCP1 is important for CNYDase activity, we expressed and purified an alanine-substituted (C161A) XCP1-His mutant. Indeed, the CNYDase activity of (C161A) XCP1-His mutant was dramatically lower than native XCP1-His (Fig. S7). Together, these data suggest that XCP1 is a caspase in *Arabidopsis*.

Importantly, we observed increased production of AtCAPE9-eYFP (~27.0 kDa) from AtPR1-eYFP in WT *Arabidopsis* lysate supplemented with Ni-NTA-purified proteins from tobacco expressing P19 plus XCP1-His versus P19 alone (Fig. 4f). To determine if XCP1-His can interact with and process AtPR1-eYFP directly, we immobilized AtPR1-eYFP on Protein A/G beads with an anti-PR1 antibody, followed by incubation Ni-NTA-purified proteins from tobacco without or with expressing XCP1-His. Incubation with purified XCP1-His increased the release of AtCAPE9-eYFP from immobilized AtPR1-eYFP compared to the control (Fig. 4g). These data suggest that XCP1 directly processes AtPR1 into AtCAPE9. Therefore, we suggest a functional name for XCP1 as ESCAPE.

XCP1/ESCAPE regulates local and systemic immunity in *Arabidopsis*

Our data so far suggest that XCP1 is ESCAPE that can generate the immune elicitor AtCAPE9 from AtPR1, so we further investigated how this enzyme regulates CNYDase activity and disease resistance of

Arabidopsis. Briefly, we used homozygous wild-type *XCP1/ESCAPE* (*ESCAPE*$^{w/w}$), and mutated *XCP1/ESCAPE* (*ESCAPE*$^{m/m}$) and heterozygous mutated *XCP1/ESCAPE* (*ESCAPE*$^{w/m}$) plants from F2 generation of WT and *xcp1* (*escape*) crossed plant (WT x *escape*) lines. We found that the reduction of the CNYDase activity and pathogen resistance in *ESCAPE*$^{m/m}$ lines as compared to *ESCAPE*$^{w/w}$ and *ESCAPE*$^{w/m}$ lines, and the pathogen infection of *ESCAPE*$^{m/m}$ lines was almost as severe as loss of AtPR1 in the plants (*atpr1* mutant) (Fig. 5a, b).

To examine pathogen-mediated regulation of AtPR1 proteolytic processing, we applied a conserved pathogen-associated molecular pattern (PAMP) elicitor, flg22, to plants expressing AtPR1-eYFP. Flg22 treatment promoted the proteolysis of AtPR1-eYFP (~44.7 kDa) and, in turn, the production of AtCAPE9-eYFP (~27.0 kDa) (Fig. 5c), suggesting that flg22 treatment promotes ESCAPE-dependent cleavage of AtPR1.

To show that ESCAPE is involved in flg22-triggered systemic immunity, we treated plants locally with flg22 and monitored CNYDase activity and disease resistance in untreated leaves. Specifically, we employed *ESCAPE*$^{w/w}$, and *ESCAPE*$^{m/m}$ F2 lines from WT x *escape* and a complement line obtained by expressing *ESCAPE-His* in the *escape* mutant (*escape/ ESCAPE-His*). We locally infiltrated flg22, and observed reduced CNYDase activity and diminished resistance to *Pst* DC3000 in the untreated leaves of the *ESCAPE*$^{m/m}$ line compared to both *ESCAPE*$^{w/w}$ and *escape/ ESCAPE-His* lines (Fig. 5d).

Discussion

In this study, we identified endogenous AtCAPE9 and showed its function in activating SA biosynthesis and an immune response. We show for the first time that AtCAPE9 is derived from the cleavage of the putative caspase substrate domain CNYD in AtPR1, in SA-treated *Arabidopsis* leaves. The aspartate residue (D150) of the CNYD domain that is immediately N-terminal to the AtCAPE9 domain is crucial for the cleavage of AtPR1-eYFP to generate AtCAPE9-eYFP in plants, indicating that AtCAPE9 production requires an aspartate-specific protease. We further demonstrated that SA treatment enhanced the endogenous production of AtCAPE9, the proteolytic cleavage of AtPR1-eYFP to produce AtCAPE9-eYFP, and CNYDase activity in plants. We found that CNYDase activity and thus AtCAPE9 production were not induced by wounding in *Arabidopsis*. However, our observation that SA both induces and is induced by AtCAPE9 suggests the existence of a positive-feedback loop to amplify SA-mediated defense responses in plants.

We found that cleavage of CNYD substrates is mediated by recognition of the CNYx motif. CNYDase activity in plant extract was specifically suppressed by the cysteine protease inhibitor E-64 and the substrate-specific inhibitor biotin-CNYD-CHO, but not by the serine protease inhibitor PMSF, consistent with a caspase activity. We successfully identified an *Arabidopsis* PLCP member XCP1 as enzyme specific for CAPE production (ESCAPE). XCP1 was identified as ESCAPE based on our discovery of the sizes of CNYDase and its overlapping gene expression pattern with AtPR1 in plant leaves. XCP1/ESCAPE and its paralog XCP2 have been reported to aid in the formation of tracheary elements (TEs) prior to the

macro-autolysis followed by vacuole and protoplast disruption[19]. These two proteases are translocated to the vacuole during the formation of TEs and released to the xylem after the breakdown of the protoplast. The XCPs loss-of-function plants *xcp1xcp2* show a delay of micro-autolysis, but do not exhibit a noticeable change in growth and developmental phenotypes, including TEs, as compared to wild-type plants. Although XCPs are not essential in growth and development, XCP1/ESCAPE has been shown to participate in basal defense functions[20]. The XCP1/ESCAPE protein and its cysteine protease activity is also a target of the pathogen effector Avr2 from *Cladosporium fulvum,* to suppress plant resistance. Together with the defense function and identification of XCP1/ESCAPE in maize xylem sap[21], it was suggested that XCP1/ESCAPE serves defense functions that are expressed and propagated in plant xylem[22].

Here, we demonstrate that XCP1/ESCAPE plays a major role in the CNYDase activity in plants, given that protein extracts from *xcp1* (*escape*) mutants were not tagged with biotin-CNYD-CHO and showed a significant loss of CNYDase activity. Purified XCP1-His (ESCAPE-His) was highly specific for the CNYD domain and its CNYDase activity was enhanced by Ca^{2+} but repressed by Zn^{2+} and E-64. Importantly, we provide strong evidence that purified ESCAPE-His directly cleaves AtPR1-eYFP to release AtCAPE9-eYFP. XCP1/ESCAPE activity was temperature sensitive, displaying optimal CNYDase activity at 22 °C, which is also optimal for growth of *Arabidopsis*. In addition, XCP1/ESCAPE displayed a K_m of 26.5 μM for the CNYD substrate, which is comparable to the K_m for human caspase-1 with the YVAD substrate (20 μM)[23]. Interestingly, the optimal pH for XCP1/ESCAPE CNYDase activity was altered by adding excess Ca^{2+}, suggesting that apoplastic pH and Ca^{2+} levels can fine-tune the production of AtCAPE9 by XCP1/ESCAPE to regulate plant immunity. We showed that XCP1/ESCAPE CNYDase activity is dependent on C161 in its putative protease active site. Both homozygous mutated *XCP1/ESCAPE* (*ESCAPE*$^{m/m}$) lines and *atpr1* mutant plants were more susceptible to pathogen infection than homozygous wild-type *XCP1/ESCAPE* (*ESCAPE*$^{w/w}$) and the heterozygous mutated *XCP1/ESCAPE* (*ESCAPE*$^{w/m}$) lines. The *atpr1* mutant showed a less resistance to the infection than the *ESCAPE*$^{m/m}$ lines, suggesting that AtPR1 may participate in defense beyond the production of AtCAPE9 or that the basal CNYDase activity in *ESCAPE*$^{m/m}$ lines may generate some AtCAPE9 from AtPR1 to support resistance. The PAMP flg22 triggered systemic CNYDase activity and antipathogen responses in *ESCAPE*$^{w/w}$ line and the ESCAPE-His complemented *escape* plants, but not in *ESCAPE*$^{m/m}$ line. Flg22 cannot elicit systemic acquired resistance (SAR) in the absence of ESCAPE, suggesting that the positive signaling feedback loop that amplifies SA production for SAR may be blocked in the *escape* mutant, likely due to the reduced production of AtCAPE9.

In summary, XCP1/ESCAPE is a plant caspase for initiating systemic immunity. The enzyme activity of XCP1/ESCAPE is cysteine-dependent, is specific for cleaving the aspartate of a four amino acid substrate domain, and can release the cytokine AtCAPE9 to activate systemic immunity. As the secretion of AtPR1 is thought to be crucial for SAR[14] and XCP1/ESCAPE has been suggested to be an apoplastic and vacuolar localized protein[19], our data suggest that PR1 is processed by XCP1/ESCAPE in the apoplast to induce SAR. The cysteine protease activity of XCP1/ESCAPE can be targeted by the effector Avr2, which

may disrupt its CNYDase activity and, in turn, the production of AtCAPE9 and the induction of SA. The temperature sensitivity of XCP1/ESCAPE activity might help to explain why pathogen-induced SA-defense responses are temperature-vulnerable[24]; lower XCP1/ESCAPE activity at higher temperatures is expected to yield less AtCAPE9 and thus diminished SA biosynthesis. Compared to the activation and secretion of immunomodulatory cytokines triggered by caspases in animals, plant PR1 acts like a pro-cytokine that is activated by XCP1/ESCAPE to produce the SAR signal AtCAPE9. As PR1 is conserved in humans[25], these findings might stimulate the search for a similar mechanism in mediating human immunity.

Methods

Plant materials and growth conditions

The wild-type (WT) plant seeds of *Arabidopsis thaliana* Columbia (Col-0, CS70000) and all T-DNA insertion mutant lines were purchased from the Arabidopsis Biological Resource Center (ABRC). All plant seeds used in this work were subjected to surface sterilization before use. The *Arabidopsis* plants grown in soil were cultivated in a growth chamber with a 10/14 h light/dark cycle (for vegetative growth and delayed flowering) or a 16/8 h light/dark cycle (for seed collection) at 22 °C under light and 20 °C under dark. The *Arabidopsis* seedlings in Murashige & Skoog (MS) agar plates were grown by sowing the seeds on MS agar plates with 1/2 × MS salts, 1% (w/v) sucrose, 0.05% (w/v) MES and adjusted with KOH to pH 5.7. These seeds on plates were incubated at 4 °C for 2 days in the dark, then cultivated at 22 °C in a growth chamber under a 16/8 h light/dark cycle for 10 days before use. Eight-week-old Col-0 plants grown in soil were used for quantifying the salicylic acid (SA) level regulated by AtCAPE9. Twelve-day-old Col-0 seedlings grown in MS agar plates were used for examining the plant pathogen resistance enhanced by AtCAPE9. Nine-week-old Col-0 plants grown in soil were used for the detection and quantification of endogenous AtCAPE9. Twelve-day-old transgenic Col-0 seedlings grown in MS agar plates expressing native (N) and alanine-substituted (D150A and P151A) AtPR1 fused to a C-terminal enhanced yellow fluorescent protein (eYFP) were used for monitoring the cleavage of AtPR1. The homozygous wild-type *XCP1/ESCAPE* (*ESCAPE*$^{w/w}$, Line #5), two heterozygous mutated *XCP1/ESCAPE* (*ESCAPE*$^{w/m}$, Line #6 and 13) and two homozygous mutated *XCP1/ESCAPE* (*ESCAPE*$^{m/m}$, Line #3 and 8) were generated from F2 generation of WT and *xcp1* (*escape*) crossed plant (WT x *escape*) lines. Genotyping the *XCP1/ESCAPE* zygosity in WT x *escape* F2 lines was illustrated in Fig. S8a. Plant leaves from nine-week-old Col-0, T-DNA insertion mutants and the complemented or crossed plants grown in soil were used to exam the CNYD-targeted protease (CNYDase) activity and plant resistance to the pathogen. *Nicotiana benthamiana* (tobacco) grown in soil at 25 °C in a walk-in growth chamber under a 16/8 h light/dark cycle for 4 weeks was used for transiently expressing the recombinant protease candidate and its mutated form. All T-DNA insertion mutants of *Arabidopsis* used in this study are shown in Table S2. All mutants and complement lines were genotyped for zygosity using allele-specific primers shown in Table S3.

DNA cloning and transformation

The cDNA sequences of *Arabidopsis* were produced via reverse transcription and the DNA fragments of target genes *AtPR1* and *XCP1* were amplified by the specific primer using Perfectread *Pfu* polymerase and the final product of XCP1 (ESCAPE) was added with the C-terminal 6x Histidine tag (HisTag) for purification purposes. The DNA products were purified using Gel/PCR DNA fragment extraction kit. The primers used for cloning are listed in Table S3.

To generate the clones carrying the sequences of interest, the amplified DNA fragment was cloned into the pCR8 entry vector using pCR™8/GW/TOPO™ TA Cloning Kit (Invitrogen). The pCR8-XCP1-His clone was transferred into a gateway vector pMDC32 carrying a dual 35S promoter. The native and two alanine-substituted (N, D150A and P151A) AtPR1 clones were transferred into pK7YWG2 carrying a single 35S promoter, using a method outlined in our previous study[26]. The C161A mutated XCP1-His clone was obtained by cloning of pMDC32-XCP1-His using a pair of point mutation primers. The mutated XCP1-His clone was inserted into the PCR8 entry clone and then transfer to the pMDC32.

To observe the proteolytic processing of AtPR1, the N, D150A, and P151A AtPR1-eYFP clones were separately transformed to WT *Arabidopsis* (Col-0) plants to produce a stable transgenic line (T3 generation lines were used in this study). To express the XCP1-His protein, the 2x35S::XCP1-His was transformed into tobacco plants for transient expression and the proteins extracted from tobacco leaves were purified by Ni-NTA column. The ESCAPE-His complemented *escapes* mutant (*escape/ESCAPE-His*) lines were obtained from the T3 generation of the *xcp1* (*escape)* mutant transformed with native promoter driven *XCP1-His* (*ESCAPE-His*). The expression of *ESCAPE* in the WT, *escape* and *escape/ESCAPE-His* plants was quantified by RT-PCR (Fig. S8b). All the binary vectors were transformed into *Agrobacterium tumefaciens* strain GV3101 using electroporation[27]. *Arabidopsis thaliana* (Col-0) and *Nicotiana benthamiana* plants were transformed by the floral dipping method and agroinfiltration using *Agrobacterium tumefaciens*-mediated transformation system, respectively[28].

Peptide or phytohormone treatment

For detecting the SA concentrations regulated by AtCAPE9, eight-week-old Col-0 plants sprayed with water or an aqueous solution of 250 nM synthetic AtCAPE9. For measuring the bacterial growth of the plants treated with AtCAPE9, twelve days-old Col-0 seedlings were immersed in 1/2 MS medium adding with water or an aqueous solution of 250 nM synthetic AtCAPE9 for 6 h in dark before pathogen inoculation. To detect and quantify endogenous AtCAPE9 production, nine-week-old Col-0 plants untreated or treated with 1 mM SA in 0.0015% Silwet L-77 were used. To monitor the proteolytic processing of AtPR1 regulated by 2,6-dichloroisonicotinic acid (INA) and SA, twelve-day-old seedlings of AtPR1-eYFP transgenic lines were immersed in 10 mM $MgSO_4$ (Mock), 60 μM SA in 10 mM $MgSO_4$, INA in 10 mM $MgSO_4$ for 5, 30 and 60 min. To monitor the proteolytic processing of AtPR1 regulated by flg22, twelve-day-old seedlings of AtPR1-eYFP transgenic lines were immersed in 10 mM $MgSO_4$ (Mock) or 500 nM synthetic flg22 in 10 mM $MgSO_4$ for 4 and 24 h. To monitor the CNYDase activity triggered by wounding, INA, or SA in plants, eight-week-old Col-0 plants were wounded by forceps, sprayed with 10 mM $MgSO_4$ as

mock, 60 μM SA in 10 mM $MgSO_4$ or INA in 10 mM $MgSO_4$ for 24 h. To examine the role of ESCAPE in flg22-triggered systemic immunity, the selected leaves of plants were infiltrated with 500 nM flg22 in 10 mM $MgSO_4$ or 10 mM $MgSO_4$ (Mock) for 48 h treatment and their corresponding untreated leaves were used as the systemic leaves.

Pathogen infection

The bacterial pathogen *Pseudomonas syringae* pv. tomato DC3000 (*Pst* DC3000) was grown on King's B (KB) agar medium containing 50 mg/L rifampicin for 2 days at 28 °C. Before the challenge, the bacteria were cultured in KB liquid medium at 28 °C with 230 rpm shaking overnight. The bacteria were pelleted by centrifugation and resuspended in 10 mM $MgSO_4$ at A600 = 0.2 (about 10^8 cfu/ml). Twelve-day-old seedlings of *Arabidopsis* were immersed with a mock or peptide solution for 6 h, then immersed into a diluted suspension of ~10^5 cfu/ml *Pst* DC3000 in 10 mM $MgSO_4$ containing 0.005% Silwet L-77. The bacterial populations were measured after 5 days of inoculation, represented as log colony-forming units (Log CFU) per seedling. Nine-week-old adult plants were dipped into a diluted suspension of ~10^7 cfu/ml *Pst* DC3000 in 10 mM $MgSO_4$ containing 0.005% Silwet L-77 for 1 min. The bacterial populations were calculated from leaf discs after 7 days inoculation, represented as Log CFU per leaf disc (cm^2) according to a method outlined previously[13]. To examine the flg22-triggered systemic immunity, eight-week-old plants were locally infiltrated by 500 nM flg22 in 10 mM $MgSO_4$ or 10 mM $MgSO_4$ (Mock) for 48 h, then dipped into a diluted suspension of ~10^7 cfu/ml *Pst* DC3000 in 10 mM $MgSO_4$ and 0.005% Silwet L-77. The bacterial populations were calculated from leaf discs after 5 days of inoculation, represented as Log CFU per leaf disc (cm^2).

Endogenous peptide isolation and detection

Nine-week-old *Arabidopsis* plants treated with or without 1 mM SA with 0.0015% Silwet L-77 solution were collected and individually ground into powder under liquid nitrogen using a homogenizer (Nissei ACE Homogenizer AM-5). Frozen leaf powder (50 g) was dissolved in 150 ml of 1% TFA and homogenized to leaf juice using a blender for 2 minutes. The leaf juice was filtered through four layers of cheesecloth and one layer of Miracloth (Calbiochem). The filtrated leaf juice was then centrifuged at 10,000 × g for 20 minutes at 4 °C. The supernatant was adjusted to pH 4.5 with 10 N NaOH and centrifuged at 10,000 × g for 20 minutes at 4 °C. Then the supernatant was re-adjusted to pH 2.5 using TFA and 50 μg tryptic β-casein peptides were added to the supernatant as an internal control for peptide abundance normalization. To avoid the trypsin residue reacting with the endogenous proteins or peptides, the tryptic β-casein peptides were acidified by TFA and purified using C18 Sep-pak (20 mg) cartridge (Waters). To purify the supernatant, the customized C18 Sep-pak (20 g) cartridge was used and first equilibrated by 60 ml 0.1% TFA. The supernatant was loaded into the Sep-Pak cartridge, washed with 100 ml 0.1% TFA and eluted by 150 ml of 60% methanol in 0.1% TFA. The eluted solution was vacuum-evaporated to remove methanol using a vacuum centrifugation concentrator (miVac Duo Concentrator, Genevac) to dryness[13]. The dried crude extract was dissolved in 1 ml of 0.1% TFA, centrifuged at 10,000 ×

g for 10 minutes at 4 °C and filtered through a 0.45 μm filter (Millipore) before peptide fractionation. The filtrated peptide extract was injected into a Superdex Peptide 10/300 column (GE Healthcare) and eluted by 0.5 ml/min of 0.1% TFA with 1 fraction/min for collecting the peptide fractions and evaporated to dryness by a vacuum centrifugal concentrator. Each fraction was purified by C_{18} ZipTip (Merck Millipore) for LC-MS/MS analysis. To identify the AtCAPE9 from endogenous peptides, the LC-MS/MS operated in data-dependent acquisition (DDA) mode was used. To quantify the AtCAPE9 abundance in *Arabidopsis*, the LC-MS/MS operated in selected reaction monitoring (SRM) mode targeting on the fragmentation transitions of AtCAPE9 was applied.

Phytohormone Extraction

After peptide treatment, the metabolites were extracted from leaf tissues for phytohormone quantitation. The extraction procedure was modified from a previously published protocol[29]. The leaf tissues (about 0.4 g fresh weight) were ground into a powder under liquid nitrogen and transferred to a 50 ml screw-cap tube. The frozen leaf powder was dissolved in 4 ml extraction solvent and d_6-SA (2 ng to 0.4 g leaf tissue) added as internal standards. The samples were extracted by rotating at a speed of 100 rpm at 4 °C for 30 min and then 8 ml dichloromethane was added to each sample and shaken at 100 rpm at 4 °C for 30 min. The samples were centrifuged at 13,000 × g at 4 °C for 5 min, and two phases were formed. The lower phase was transferred carefully into a new tube and evaporated to dryness by a vacuum centrifugal concentrator. The dried samples were dissolved in 300 μl methanol, mixed well and centrifuged at 10,000 × g at 4 °C for 5 min and then the supernatant was transferred to the sample vial for targeted quantitation analysis using LC-MS/MS.

Targeted Peptide and Phytohormone Quantitation using LC-MS/MS

For targeted peptide quantitation, a linear ion trap-orbitrap mass spectrometer (Orbitrap Elite, Thermo Fisher Scientific) coupled online with a nanoUHPLC system (nanoACQUITY UPLC, Waters) was used. The nanoUHPLC method was followed by our previous study[13, 30]. The mass spectrometer was operated in the positive ion mode and set to one full FT-MS scan (m/z 400-1600) with 60,000 resolution and switched to one ion trap analysis in selected reaction monitoring (SRM) mode. For SRM targeted on AtCAPE9, the doubly charged AtCAPE9 precursor ion (m/z 668.84) was selected for fragmentation and product ions m/z of 1058.52, 529.76 and 930.44 were monitored. The relative abundances of AtCAPE9 in untreated and SA-treated samples were estimated by combining SRM peak areas of product ions. To quantify the abundance of AtCAPE9, one doubly charged tryptic β-casein peptide (m/z 1031.42) was selected for fragmentation and product ions m/z of 1105.44, 1361.61 and 747.34 were monitored. The normalized abundance of AtCAPE9 was calculated by the peak area of fragment ions and normalized with the abundance of a selected tryptic β-casein peptide.

For phytohormone quantitation, a linear ion trap-orbitrap mass spectrometer (Orbitrap Elite, Thermo Fisher Scientific) coupled online with a UHPLC system (ACQUITY UPLC, Waters) was used. The phytohormones were separated by an HSS T3 column (Waters) using gradients of 0.5-25% ACN at 0-2

min, 25-75% ACN at 2-7 minutes and 75-9.5% ACN at 7-7.5 minutes. The mass spectrometer was operated in the negative ion mode and set to one full FT-MS scan (m/z 100-600) with 60,000 resolution and switched to two FT-MS product ion scans (in 30,000 resolution) for two precursors: m/z of 137.02 (for SA), 141.05 (for d_6-SA dissociated to d_4-SA). The fragmentation reactions of m/z 137.02 to 93.03 for SA and 141.05 to 97.06 for d_4-SA were selected for quantitation. The absolute abundances of SA were calculated by the abundance of d_4-SA.

Assay for protease activity

To test the protease activity against different substrates, metals ion, and inhibitors, the substrate reaction buffer 50 mM MOPS with 0.1% CHAPS for pH 6.0 was used. To investigate the specificity of the protease, three synthetic peptides (CNYD, CNAD, and ANAD) tagged by 7-amino-4-methylcoumarin (AMC) at the C-terminus were purchased from Mission Biotech. These substrates were incubated with *Arabidopsis* protein extract or the purified XCP1-His protein in pH 6.0 reaction buffer, then the protease activity was measured through the detection of the fluorophore released from the substrates. The fluorescent signal of the released fluorophore was detected by an ELISA microplate reader (BioTek Synergy H1) using 360 nm excitation and 460 nm emission. To evaluate the effects of metal ions or inhibitors for CNYDase activity, *Arabidopsis* protein extracts were incubated with 100 mM $ZnCl_2$, $MgCl_2$, and $CaCl_2$ or 5 mM EDTA in reaction buffer for 1 h and then the CNYDase activity was measured after 5 h incubation with the substrate. The synthetic affinity aldehyde inhibitor using the CNYD sequence tagged by biotin at N-terminus and the CHO aldehyde group at C-terminus (designated as biotin-CNYD-CHO) was purchased from Biotools. To examine the effects of protease inhibitors with or without calcium activation, *Arabidopsis* protein extracts were incubated with 200 μM phenylmethanesulfonyl fluoride (PMSF) (Sigma-Aldrich), 500 μM E-64 (Sigma-Aldrich) or 100 μM biotin-CNYD-CHO in reaction buffer for 1 h with or without 100 mM $CaCl_2$ and the CNYDase activity was measured after 10 h incubation with the substrate. Dose-dependent inhibition of biotin-CNYD-CHO was examined by the CNYDase activity. The *Arabidopsis* leaf protein extracts incubated with 0, 25, 50, 100, and 200 μM biotin-CNYD-CHO for 1 h and the CNYDase activity were measured after 10 h incubation with the substrate. The proteolytic activity assay of protein extract was performed by incubating 50 μg protein extract with 25 μM substrate. The CNYDase activity of T-DNA insertion mutants of *Arabidopsis* Col-0 and the protease candidates were measured after 5 h incubation with the substrate. To study the XCP1-His activity at different pH, the substrate reaction buffer of 100 M sodium acetate with 0.1% CHAPS was used for the range of pH 4.0-5.5 and 50 mM MOPS with 0.1% CHAPS was used for the range of pH 6.0-7.5. For the enzyme kinetics of XCP1 activity at different temperatures, the V_{max} and K_m of proteolytic activity were determined by 2.5 h incubation of 1 μg purified XCP1-His with different concentration of CNYD substrate at 22, 32, or 37 °C. To determine the XCP1 activity at 22 °C, the V_{max} and K_m of proteolytic activity were determined by 10 h incubation of 0.2 μg purified XCP1-His with different concentrations of CNYD substrate.

Immunoblotting and immunoprecipitation for AtPR1-eYFP processing

For the analysis of AtPR1-eYFP processing, the samples of *Arabidopsis* WT, D150A, and P151A of AtPR1-eYFP transgenic plants were frozen in liquid nitrogen and ground into fine powder, then dissolved in the plant extraction buffer (50 mM sodium acetate with 200 mM NaCl and 3 mM DTT at pH 5.0) rotating 50 rpm for 30 min at 4 °C. Protein extract was centrifuged 15 minutes at 16,000 x g at 4 °C and the supernatant was filtered by 70 μM Nylon cell strainer (Falcon). The protein concentration was measured and taking 50 μg proteins dissolved by a loading buffer with 5x sample buffer (250 mM Tris at pH 6.8 with 50% glycerol, 5% SDS, and 0.02% bromophenol blue) and β-mercaptoethanol for heating at 95 °C for 5 min. The proteins were separated by 12.5% SDS-PAGE gels (1.0 mm) and transferred onto PVDF membranes by wet western blot. Membranes were first blocked with a 5% milk in Tris buffer saline-Tween 20 (TBST) buffer and then incubated with anti-GFP antibody (mouse, 1:1000; #11814460001, Roche) for 4 °C overnight. For detecting the recombinant proteins tagged with C-terminal 6XHis, the proteins in the transferred membrane were incubated with anti-His antibody (mouse, 1:5000; #PPT-66005-1, Biotools) at room temperature for 1 h. Protein complexes were labeled with the secondary antibody (mouse, 1:5000; # 61-6520, Thermo Fisher). For measuring the biotin-CNYD-CHO-bounded proteins, the western blot was performed by streptavidin-HRP (1:5000; #016-030-084, Jackson ImmunoResearch). All HRP-conjugated proteins were detected on the membrane with enhanced chemiluminescence (ECL) reagent kit (#193508, Biotools) reacting to the HRPs.

For the direct interaction of AtPR1-eYFP and XCP1-His, the immunoprecipitation of AtPR1-eYFP was performed by anti-AtPR1 antibody (Rabbit, #AS10687, Agrisera) immobilized on the Pierce™ Protein A/G Magnetic Beads (#88803, Thermo Fisher) and the immobilized AtPR1-eYFP proteins were incubated with the Ni-NTA purified proteins from the tobacco overexpressed P19 or P19 plus XCP1-His gene in pH 6.0 reaction buffer for 1 h. The elution of the intact AtPR1-eYFP and the proteolytic fragment of AtCAPE9-eYFP using IgG Elution Buffer, pH 2.0 (#21028, Thermo Fisher) from the Protein A/G Magnetic Beads was detected by anti-GFP antibody (mouse, 1:1000; #11814460001, Roche).

Declarations

Acknowledgements

The MS analysis was supported by the Metabolomics Facilities of the Scientific Instrument Center at Academia Sinica. This work was financially supported by the Academia Sinica (CDA-105-L03) and the Ministry of Science and Technology of Taiwan (MOST 107-2113-M-001-006). We thank Life Science Editors for editorial assistance.

Contributions

Y.-R.C. conceptualized the project and acquired funding, Y.-L.C. and Y.-R.C contributed ideas, designed experiments, Y.-L.C. identified and quantified the endogenous AtCAPE9, F.-W.L. studied the potential protease activity in plants, purified the key protease and performed most of the experiments and recorded the data, K.-T.C. operated all pathogen experiments and recorded the data, H.-Y.W. prepared all constructs and screened the plant mutants, T. E. performed the molecular docking analysis to identify enzyme

candidates. Y.-L.C analyzed the data, Y.-L.C. and Y.-R.C wrote the manuscript with help from all of the co-authors.

References

1. Salvesen, G.S., Hempel, A. & Coll, N.S. Protease signaling in animal and plant-regulated cell death. *Febs J* **283**, 2577-2598 (2016).
2. De Lorenzo, G., Ferrari, S., Cervone, F. & Okun, E. Extracellular DAMPs in Plants and Mammals: Immunity, Tissue Damage and Repair. *Trends in Immunology* **39**, 937-950 (2018).
3. Man, S.M. & Kanneganti, T.D. Converging roles of caspases in inflammasome activation, cell death and innate immunity. *Nat Rev Immunol* **16**, 7-21 (2016).
4. Woltering, E.J., van der Bent, A. & Hoeberichts, F.A. Do plant caspases exist? *Plant Physiol.* **130**, 1764-1769 (2002).
5. Bonneau, L., Ge, Y., Drury, G.E. & Gallois, P. What happened to plant caspases? *Journal of experimental botany* **59**, 491-499 (2008).
6. Coll, N.S. et al. Arabidopsis Type I Metacaspases Control Cell Death. *Science* **330**, 1393-1397 (2010).
7. Dickman, M., Williams, B., Li, Y.R., Figueiredo, P. & Wolpert, T. Reassessing apoptosis in plants. *Nat Plants* **3**, 773-779 (2017).
8. Vartapetian, A.B., Tuzhikov, A.I., Chichkova, N.V., Taliansky, M. & Wolpert, T.J. A plant alternative to animal caspases: subtilisin-like proteases. *Cell Death Differ* **18**, 1289-1297 (2011).
9. Chichkova, N.V. et al. A plant caspase-like protease activated during the hypersensitive response. *Plant Cell* **16**, 157-171 (2004).
10. Gust, A.A., Pruitt, R. & Nurnberger, T. Sensing Danger: Key to Activating Plant Immunity. *Trends Plant Sci.* **22**, 779-791 (2017).
11. Chen, Y.L. et al. Quantitative peptidomics study reveals that a wound-induced peptide from PR-1 regulates immune signaling in tomato. *Plant Cell* **26**, 4135-4148 (2014).
12. Gibbs, G.M., Roelants, K. & O'Bryan, M.K. The CAP superfamily: cysteine-rich secretory proteins, antigen 5, and pathogenesis-related 1 proteins--roles in reproduction, cancer, and immune defense. *Endocr. Rev.* **29**, 865-897 (2008).
13. Chen, Y.L. et al. Quantitative Peptidomics Study Reveals That a Wound-Induced Peptide from PR-1 Regulates Immune Signaling in Tomato. *Plant Cell* **26**, 4135-4148 (2014).
14. Wang, D., Weaver, N.D., Kesarwani, M. & Dong, X.N. Induction of protein secretory pathway is required for systemic acquired resistance. *Science* **308**, 1036-1040 (2005).
15. Misas-Villamil, J.C., van der Hoorn, R.A. & Doehlemann, G. Papain-like cysteine proteases as hubs in plant immunity. *New Phytol* **212**, 902-907 (2016).
16. Klemencic, M. & Funk, C. Evolution and structural diversity of metacaspases. *J Exp Bot* **70**, 2039-2047 (2019).

17. Toufighi, K., Brady, S.M., Austin, R., Ly, E. & Provart, N.J. The Botany Array Resource: e-Northerns, Expression Angling, and promoter analyses. *The Plant journal : for cell and molecular biology* **43**, 153-163 (2005).
18. Funk, V., Kositsup, B., Zhao, C. & Beers, E.P. The Arabidopsis xylem peptidase XCP1 is a tracheary element vacuolar protein that may be a papain ortholog. *Plant Physiol.* **128**, 84-94 (2002).
19. Avci, U., Earl Petzold, H., Ismail, I.O., Beers, E.P. & Haigler, C.H. Cysteine proteases XCP1 and XCP2 aid micro-autolysis within the intact central vacuole during xylogenesis in Arabidopsis roots. *The Plant journal : for cell and molecular biology* **56**, 303-315 (2008).
20. van Esse, H.P. et al. The Cladosporium fulvum virulence protein Avr2 inhibits host proteases required for basal defense. *Plant Cell* **20**, 1948-1963 (2008).
21. Alvarez, S. et al. Characterization of the maize xylem sap proteome. *Journal of proteome research* **5**, 963-972 (2006).
22. Petzold, H.E., Zhao, M. & Beers, E.P. Expression and functions of proteases in vascular tissues. *Physiol. Plant.* **145**, 121-129 (2012).
23. Fassy, F. et al. Enzymatic activity of two caspases related to interleukin-1beta-converting enzyme. *Eur J Biochem* **253**, 76-83 (1998).
24. Huot, B. et al. Dual impact of elevated temperature on plant defence and bacterial virulence in Arabidopsis. *Nat Commun* **8**, 1808 (2017).
25. Murphy, E.V., Zhang, Y., Zhu, W. & Biggs, J. The human glioma pathogenesis-related protein is structurally related to plant pathogenesis-related proteins and its gene is expressed specifically in brain tumors. *Gene* **159**, 131-135 (1995).
26. Chien, P.S., Nam, H.G. & Chen, Y.R. A salt-regulated peptide derived from the CAP superfamily protein negatively regulates salt-stress tolerance in Arabidopsis. *Journal of experimental botany* **66**, 5301-5313 (2015).
27. Karimi, M., Inze, D. & Depicker, A. GATEWAY((TM)) vectors for Agrobacterium-mediated plant transformation. *Trends in Plant Science* **7**, 193-195 (2002).
28. Zhang, X.R., Henriques, R., Lin, S.S., Niu, Q.W. & Chua, N.H. Agrobacterium-mediated transformation of Arabidopsis thaliana using the floral dip method. *Nature protocols* **1**, 641-646 (2006).
29. Pan, X., Welti, R. & Wang, X. Quantitative analysis of major plant hormones in crude plant extracts by high-performance liquid chromatography-mass spectrometry. *Nature protocols* **5**, 986-992 (2010).
30. Chen, C.J., Chen, W.Y., Tseng, M.C. & Chen, Y.R. Tunnel frit: a nonmetallic in-capillary frit for nanoflow ultra high-performance liquid chromatography-mass spectrometryapplications. *Analytical chemistry* **84**, 297-303 (2012).

Figures

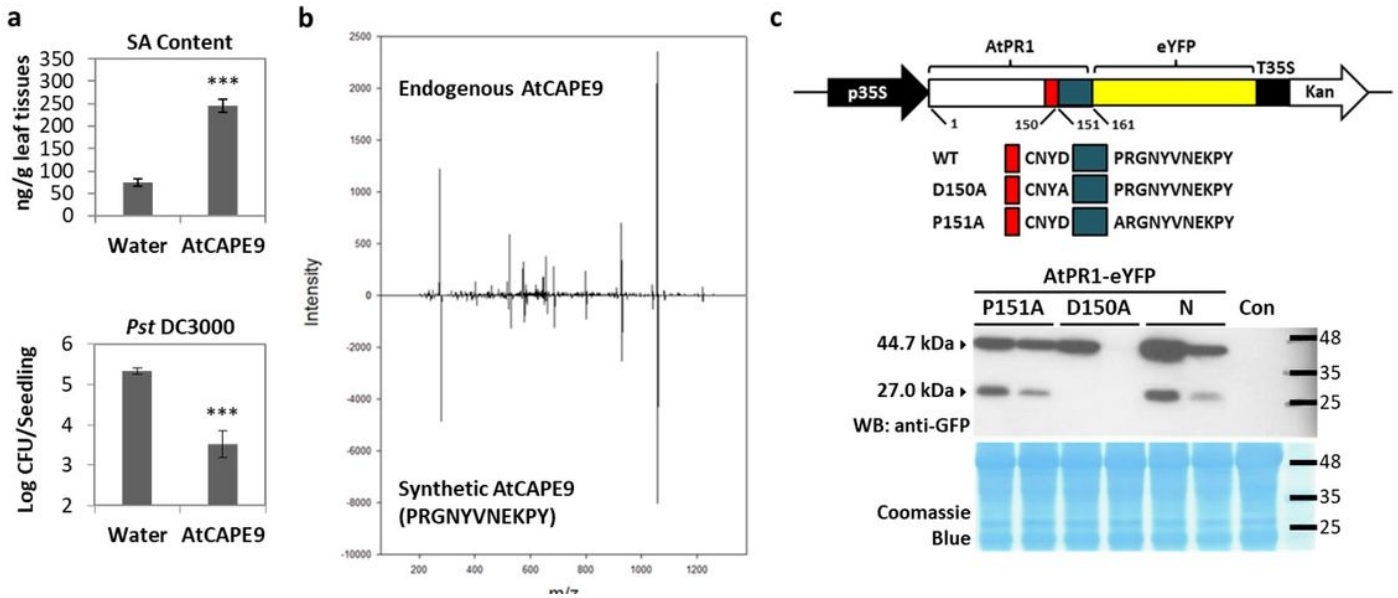

Figure 1

Bioactivity and endogenous production of AtCAPE9 through proteolysis of PR1 in Arabidopsis. (a) The SA concentrations and the growth of Pst DC3000 in Arabidopsis treated with water or AtCAPE9. The SA concentration in the plants was quantified by LC-MS/MS with spiked deuterium-labeled SA standard. Values are means ± SD of biological replicates (n=3). Each replicate was obtained from pooled tissues of three plants. Log colony-forming units (Log CFU) of Pst DC3000 was measured after 5 days of inoculation. Values are means ± SD of biological replicates (n=3). Each replicate was obtained from pooled tissues of six seedlings. P values were calculated by unpaired t-test (***, $P < 0.001$). (b) The MS/MS spectra of the endogenous and synthetic AtCAPE9. The endogenous AtCAPE9 was extracted from the plants sprayed with SA. (c) Immunoblot of the native (N) or alanine-substituted (D150A or P151A) AtPR1 fused to enhanced yellow fluorescent protein (eYFP) expressed in Arabidopsis, the Arabidopsis without expression AtPR1-eYFP was used as control (Con). A schema representing three constructs for each transgenic line is illustrated at the top of the panel. The sizes of intact AtPR1-eYFP (N, D150A, and P151A) proteins and the AtCAPE9-eYFP fragment were estimated to be ~44.7 and ~27.0 kDa, respectively, detected by western blotting with an anti-GFP antibody. Coomassie Blue staining shows total protein loaded.

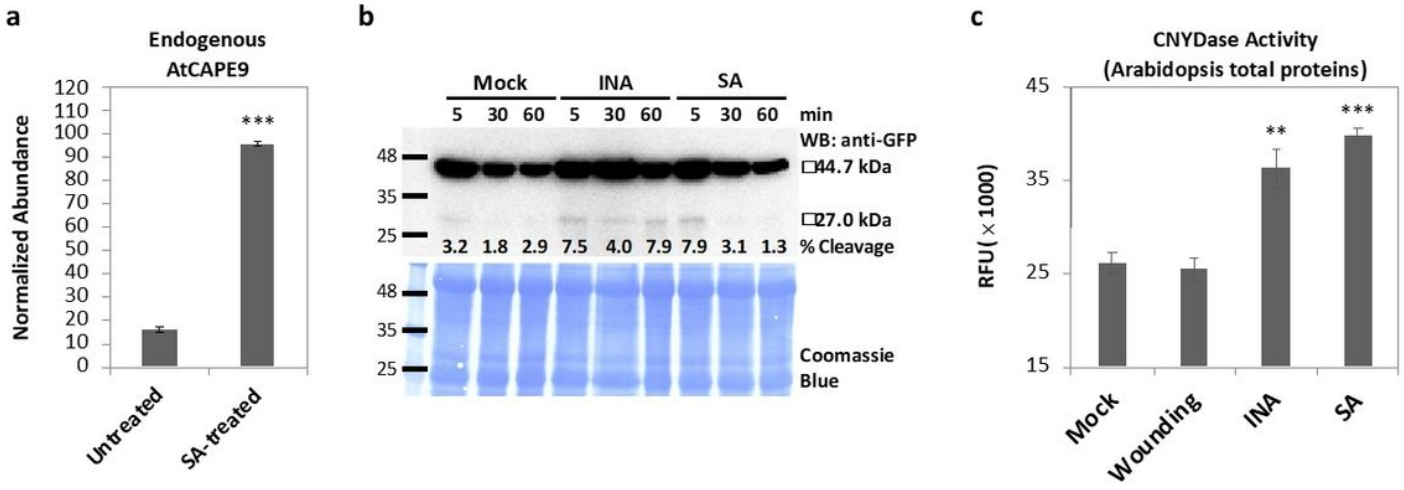

Figure 2

Induction of AtCAPE9 production, AtPR1-eYFP cleavage and CNYDase activity by SA or SA functional analogue INA. (a) The abundance of endogenous AtCAPE9 in Arabidopsis leaves with or without SA treatment. The abundance of AtCAPE9 was quantified and normalized to the abundance of a selected peptide signal from spiked tryptic β-casein using LC-MS/MS. Values are means ± SD of three technology replicates (n=3). Each replicate was obtained from the analysis of a peptide mixture extracted from 50 g leaf tissues. (b) Immunoblot of protein extracts from AtPR1-eYFP transgenic plant seedlings treated with SA or INA. The seedlings were immersed in medium with 10 mM MgSO4 (Mock), 60 mM INA in 10 mM MgSO4 (INA), or 60 mM SA in 10 mM MgSO4 (SA) for 5, 30, and 60 min. The sizes of the intact AtPR1-eYFP and the putative AtCAPE9 fragment were estimated to be ~44.7 and ~27.0 kDa, respectively, detected by the anti-GFP. The percentage of the AtPR1-eYFP cleavage (% cleavage) was calculated by the band intensity of AtCAPE9-eYFP divided by the sum of the AtPR1-eYFP and AtCAPE9-eYFP band intensities [(AtCAPE9-eYFP)/(AtPR1-eYFP +AtCAPE9-eYFP)]. Coomassie Blue staining shows total protein loaded. (c) CNYDase activity of the protein extract in wild-type (WT) Arabidopsis plants. The plants were sprayed with MgSO4 (Mock), wounded, or treated with MgSO4 plus INA or SA. Lysate was collected 24 h later. The proteolytic activity assay was performed by incubating 50 µg protein extract with 25 µM Ac-CNYD-AMC substrate. RFU of the cleaved fluorophore was measured after 10 h incubation with the substrate. Values are means ± SD of biological replicates (n=3). Each replicate was obtained from pooled tissues of three plants. P values were calculated by unpaired t-test (**, $P < 0.01$; ***, $P < 0.001$).

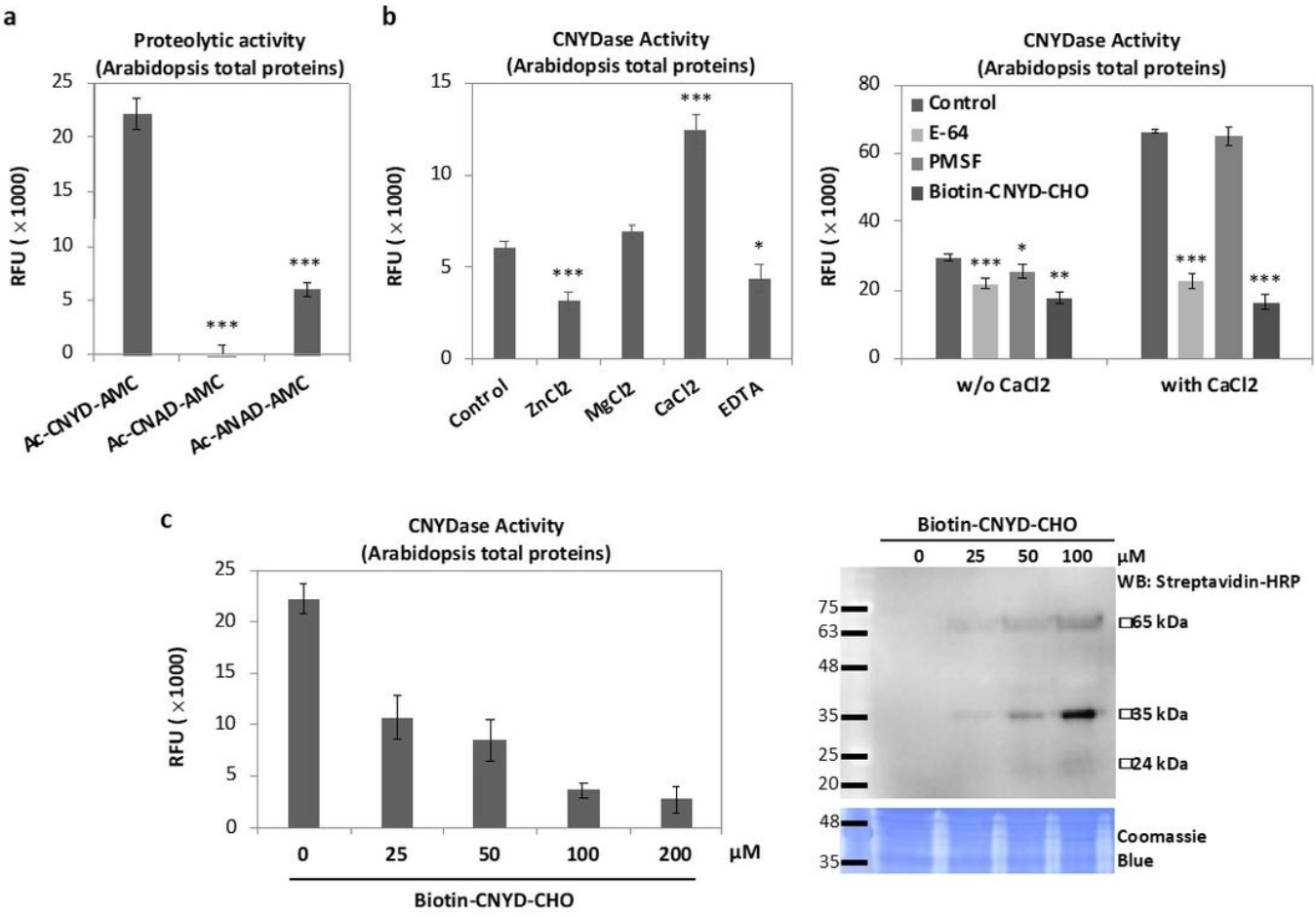

Figure 3

Proteolytic specificity of CNYD motif and the properties of CNYD-targeted protease in Arabidopsis. (a) Proteolytic activity of Arabidopsis protein extracts on three fluorogenic protease substrates (CNYD, CNAD, and ANAD). Relative fluorescent units (RFU) of the cleaved fluorophore was measured after 5 h incubation with the substrate. (b) CNYDase activity of Arabidopsis protein extracts supplemented with 100 mM of ZnCl2, MgCl2 or CaCl2, or 5 mM of EDTA (left) or with PMSF, E-64, or biotin-CNYD-CHO, with or without CaCl2, (right) for 1 h prior to substrate incubation. RFU of the cleaved fluorophore was measured after 5 h (left) or 10 h (right) incubation with the substrate. (c) CNYDase activity and western blot of biotinylated proteins from Arabidopsis protein extracts incubated with different concentrations of biotin-CNYD-CHO. CNYDase activity of the protein extract was measured by RFU of the cleaved fluorophore after 10 h incubation with the substrate (left). Each assay was performed by incubating 50 μg protein extract with 25 μM substrate. Values are means ± SD of biological replicates (n=3). Each replicate was obtained from pooled tissues of three plants. P values were calculated by unpaired t-test (*, $P < 0.05$; **, $P < 0.01$; ***, $P < 0.001$). Biotinylated proteins were detected by western blotting with streptavidin-HRP and Coomassie Blue staining shows total protein loaded (right).

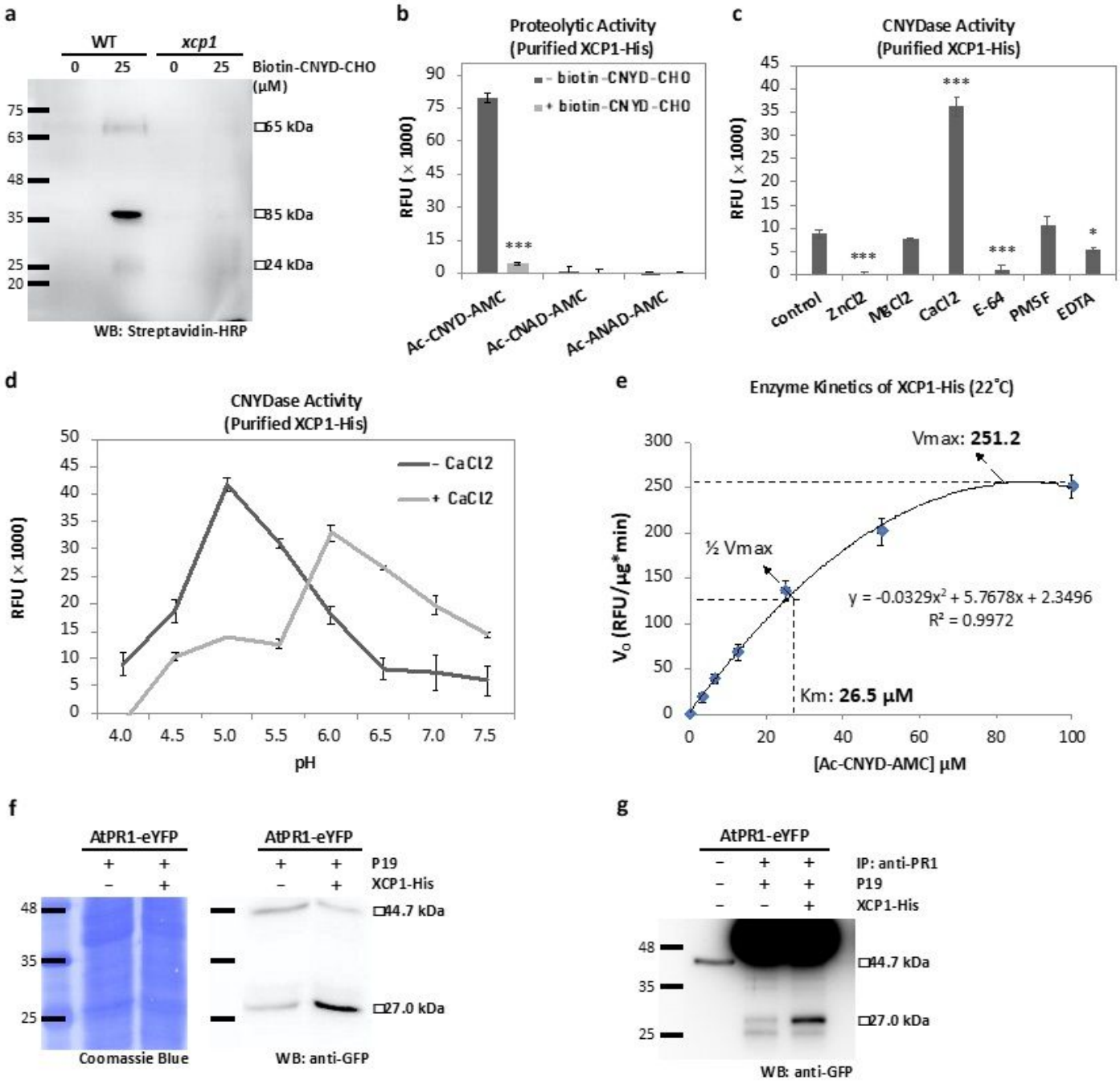

Figure 4

Characterization of the enzyme specific for CAPE production (ESCAPE) by CNYDase activity and interaction with AtPR1-eYFP. (a) Western blot of biotinylated proteins from Arabidopsis wild-type (WT) and xcp1 extracts with or without addition of biotin-CNYD-CHO. The biotinylated proteins were detected with streptavidin-HRP. (b) Proteolytic activity of purified XCP1-His on three fluorogenic protease substrates (CNYD, CNAD, and ANAD) with or without adding biotin-CNYD-CHO. Proteolytic activity of purified XCP1-His was measured by RFU of the cleaved fluorophore after 10 h incubation with the substrate. (c) CNYDase activity of purified XCP1-His supplemented with ZnCl2, MgCl2, CaCl2, E-64, PMSF, or EDTA for 1 h before substrate incubation. RFU of the cleaved fluorophore was measured after 10 h

incubation with the substrate. (d) The CNYDase activity-pH profile of purified XCP1-His, with or without adding CaCl2. RFU of the cleaved fluorophore was measured after 10 h incubation with the substrate. Each proteolytic activity assay for purified XCP1-His was performed by incubating 1 µg protein with 25 µM substrate. Values are means ± SD of biological replicates (n=3). Each replicate was obtained by using 5-7 tobacco plants overexpressed XCP1-His transiently. P values were calculated by unpaired t-test (*, P < 0.05; **, P < 0.01; ***, P < 0.001). (e) The enzyme kinetics of purified XCP1-His for CNYD substrate. The Vmax and Km of XCP1-His proteolytic activity were determined by 10 h incubation of 0.2 µg purified XCP1-His with different concentrations of CNYD substrate at 22 °C. (f) Immunoblots of the protein extracts from Arabidopsis AtPR1-eYFP transgenic plants with addition of the Ni-NTA purified proteins from the tobacco overexpressed P19 or P19 plus XCP1-His gene. AtPR1-eYFP were detected with anti-GFP antibodies. Coomassie Blue staining shows total protein loaded. (g) Immunoblot of the immobilized AtPR1-eYFP with addition of the Ni-NTA purified proteins from the tobacco overexpressed P19 or P19 plus XCP1-His gene. Protein extracts from Arabidopsis AtPR1-eYFP transgenic plants were immunoprecipitated with anti-PR1 (IP: anti-PR1) before incubation with XCP1-His. For both Fig. 4f and 4g, the sizes of intact AtPR1-eYFP and AtCAPE9-eYFP were estimated to be ~44.7 and ~27.0 kDa, respectively, detected by the anti-GFP.

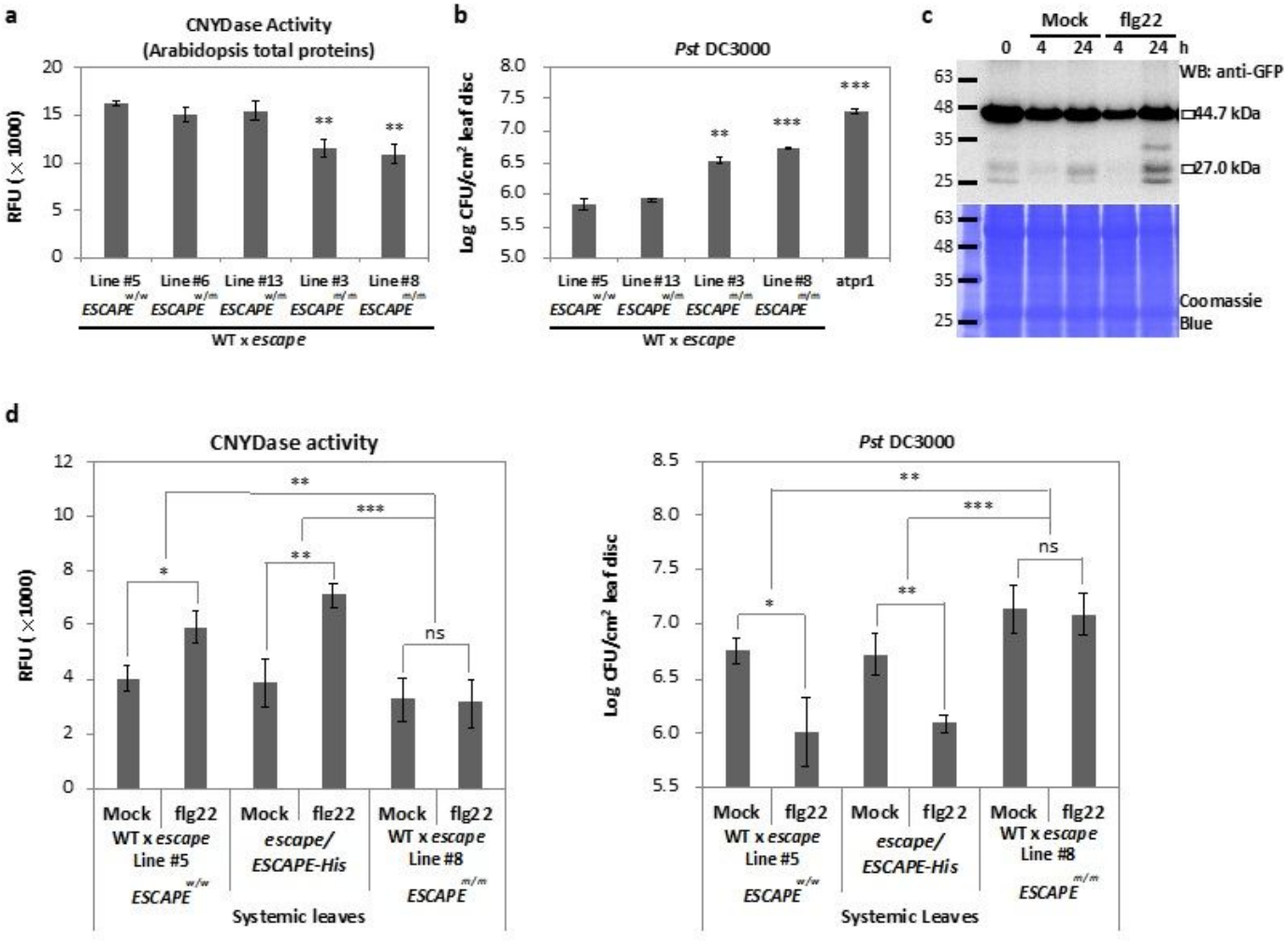

Figure 5

Role of ESCAPE in regulating Arabidopsis immunity. (a) CNYDase activity of Arabidopsis protein extracts from F2 generation of WT and xcp1 (escape) Arabidopsis crossed plant (WT x escape) lines, including one homozygous wild-type XCP1/ESCAPE (ESCAPEw/w, Line #5), two heterozygous mutated XCP1/ESCAPE (ESCAPEw/m, Line #6 and 13) and two homozygous mutated XCP1/ESCAPE (ESCAPEm/m, Line #3 and 8) lines. (b) Pst DC3000 growth in atpr1 and F2 generation of WT x escape lines, including one ESCAPEw/w (Line #5), one ESCAPEw/m (Line #13) and two ESCAPEm/m (Line #3 and 8) lines. Log colony-forming units (Log CFU) of Pst DC3000 was measured after 7 days of inoculation. (c) Immunoblot of the protein extracts from Arabidopsis AtPR1-eYFP transgenic plant seedlings treated with flg22. The seedlings were immersed in medium with MgSO4 (Mock) or MgSO4 plus flg22 for 4 or 24 h. The sizes of intact AtPR1-eYFP and the AtCAPE9 fragment were estimated to be ~44.7 and ~27.0 kDa, respectively, detected by the anti-GFP. Coomassie Blue staining shows total protein loaded. (d) The CNYDase activity and the growth of Pst DC3000 in the systemic leaves of ESCAPEw/w (Line #5), the escape complemented by expression ESCAPE-His (escape/ESCAPE-His), and ESCAPEm/m (Line #8) lines of Arabidopsis locally treated with flg22. Log colony-forming units (Log CFU) of Pst DC3000 was measured after 5 days of inoculation. Each proteolytic activity assay was performed by incubating 50 µg protein extract with 25 µM substrate. Relative fluorescent units (RFU) of the cleaved fluorophore was measured after 5 h incubation with the substrate. Values are means ± SD of biological replicates (n=3). Each replicate was obtained by pooling plant tissues of three plants. P values were calculated by the unpaired t-test (*, $P < 0.05$; **, $P < 0.01$; ***, $P < 0.001$).

Supplementary Files

This is a list of supplementary files associated with this preprint. Click to download.

- SupplementaryMaterials.pdf